

TR - H - 197

**Associative memory based on
parametrically
coupled chaotic elements**

Shin Ishii

Masa-aki Sato

1996. 7. 8

ATR人間情報通信研究所

〒619-02 京都府相楽郡精華町光台2-2 ☎ 0774-95-1011

ATR Human Information Processing Research Laboratories

2-2, Hikaridai, Seika-cho, Soraku-gun, Kyoto 619-02 Japan

Telephone: +81-774-95-1011

Facsimile: +81-774-95-1008

© (株)ATR人間情報通信研究所

Associative memory based on parametrically coupled chaotic elements

Shin Ishii Masa-aki Sato

ATR Human Information Processing Research Laboratories

2-2 Hikaridai, Seika-cho, Soraku-gun, Kyoto 619-02, Japan

(TEL) +81 774 95 1069 (FAX) +81 774 95 1008

(E-mail) ishii@hip.atr.co.jp

Abstract

In this paper, we propose an associative memory system based on parametrically coupled chaotic elements. The proposed system is obtained by adding a new parameter control to our previously proposed system. A chaotic activity in the early association stage makes an efficient association over the memories that are stored by means of an autocorrelational learning. When the system successfully recalls the target memory, the system's motion is dominated by a spatially coherent oscillation, while unstable motions remain when the system fails to make the association. In addition, the system has a large memory capacity. A comparison between the proposed system and an approach with a nonmonotonic output function is also shown.

Acknowledgement

The author would like to thank Masato Okada of Osaka University for his valuable comments and suggestions.

1 Introduction

In this paper, we propose an associative memory system based on parametrically coupled chaotic elements. In the system, a chaotic activity in the early association stage makes an efficient association over the memories that are stored by means of an autocorrelational learning. When the system successfully recalls the target memory, the system's motion is dominated by a spatially coherent oscillation, while unstable motions remain when the system fails to make the association. In addition, the system has a large memory capacity.

A biological neural network, i.e., a brain, is an ensemble of a large number of nonlinear and analog neurons, whose connections are asymmetric and highly structural. In such a complex system, one can naturally expect complex dynamics, including oscillations and chaotic activities, to occur. In the cat visual cortex, for example, stimulus-specific synchronized oscillations have been reported by Eckhorn et al. (1988) and Gray and Singer (1989). Skarda and Freeman (1987) investigated oscillations of EEG (electroencephalogram) in the rabbit olfactory system, and reported that almost periodic activity occurs for a perceptible specific odor, while chaotic activity occurs for a novel odor. This result implies that a rabbit memorizes an odor as a spatially patterned oscillation and chaos represents the state of "I don't know." Babloyantz and Destexhe (1986) analyzed human EEG in various mental states, and suggested that chaos has a role in making a response to external stimuli. These physiological studies imply that oscillatory and chaotic activities in biological neural networks are relevant to their information-processing function.

It is considered that the above-mentioned oscillatory and chaotic activities mainly originate from the network's asymmetric connections. Based on this assumption, many nonequilibrium neural network models have been studied, whose spatiotemporal complexity is attributed to the network's mutual excitatory and inhibitory (E-I) connections (Baird, 1986; Li & Hopfield, 1989; Freeman et al., 1988; Yao & Freeman, 1990; Tsuda, 1992). A similar approach is based on a network whose component is a pair of elements connected to one another by E-I connections (Wang et al., 1990; König & Schillen, 1991; Schillen & König, 1991; Grossberg & Somers, 1991). Each component works as an oscillator due to the E-I connections. All of the above-mentioned models intend to "mimic" biological neural network models, though further breakthroughs are needed to properly achieve this. The dynamics of neural network models with asymmetric connections has been investigated theoretically (Amari, 1972a; Amari, 1972b; Sompolinsky & Kanter, 1986; Babcock & Westervelt, 1987; Sompolinsky et al., 1988; Riedel et al., 1988).

From a macroscopic viewpoint, there have been many studies on networks consisting of oscillatory or chaotic elements (Kaneko, 1989; Kaneko, 1990; Aihara et al., 1990; Inoue & Nagayoshi, 1991; Kuramoto, 1991; Lumer & Huberman, 1992), where oscillatory and chaotic activities are mainly attributed to a single element's behavior. Chaotic neural network models among them are biologically motivated. A single neuron, e.g., a squid giant axon, experimentally exhibits chaotic activities (Holden et al., 1982; Matsumoto et al., 1987). The Hodgkin-Huxley equations, which quantitatively describe the ionic currents of the squid giant axon, also exhibit chaotic responses. Based on these observations, Aihara et al. (1990) proposed a chaotic neural network model whose element exhibits chaotic behavior due to its refractoriness and output nonlinearity.

Kaneko (1989; 1990) proposed several spatiotemporal chaotic models. His models are

based on coupled chaotic elements, where each element evolves in time according to the logistic map, and the couplings are of the nearest neighbor type (Kaneko, 1989), or of the global coupling type (Kaneko, 1990). The global coupling model is called the "Globally Coupled Map (GCM)," and many interesting characteristics, such as hidden coherence in turbulent states (Kaneko, 1992), have been reported. However, there have yet been no studies applying such interesting characteristics to engineering information-processing problems.

From an engineering viewpoint, it is important to implement information processing similar to that in the human brain. Let us consider the associative memory (Kohonen, 1977), which has been utilized in many engineering fields such as pattern recognition and database retrieval. Associative memory is also considered to have an important role in the hippocampus (Treves & Rolls, 1992).

Autocorrelation associative memory models were independently proposed by Nakano (1972), Anderson (1972), and Kohonen (1972). Hopfield (1982; 1984) pointed out the relation of the autocorrelation associative memory model to binary spin systems, and introduced asynchronous dynamics in which an association process corresponds to a minimization of the network's Lyapunov function. In this sense, his model employs equilibrium dynamics. He employed binary state variables (Hopfield, 1982) and analog variables (Hopfield, 1984). The analog model is equivalent to the mean-field-theory (Peterson & Anderson, 1987) of the Boltzmann machine. Hopfield (1982) also showed by computer simulations that his binary model with N neurons can store about $0.15N$ memory patterns, and if the number of memories exceeds that value all of the memories become unstable. Amit et al. (1985a; 1985b) applied the replica theory (Sherrington & Kirkpatrick, 1975) for analyzing spin-glass systems to the binary Hopfield model. They showed that there are equilibria near the stored memories when the number of memories is smaller than $0.138N$ and they become unstable when the number exceeds the capacity. The replica theory was also applied to the analog Hopfield model, and similar results were obtained (Shiino & Fukai, 1990; Kühn et al., 1991). Peretto (1988) gave another approach based on signal-to-noise analysis. Amari and Maginu (1988) investigated the recalling process based on the neuro dynamical theory, and obtained the memory capacity of $0.16N$. This result is a little larger than those of the other methods, due to the fact that the theory only considers the correlation between the signal and the crosstalk for a single evolution step. If longer-term correlations are considered, the result coincides with those of the other methods (Okada, 1995). It should be noted that the memory capacity values obtained by the above-mentioned methods allow a small discrepancy between the stored pattern and the recalled pattern. If it is not allowed, the capacity is asymptotically $N/(2 \log N)$ (Weisbuch & Fogelman-Soulié, 1985; McEliece et al., 1987), which is no longer proportional to the number of neurons.

Morita (1993) showed by computer simulations that the memory capacity of the Hopfield model is noticeably expanded by replacing the conventional Heaviside or sigmoidal output function with a nonmonotonic output function. He reported that the memory capacity becomes about $0.32N$. Yoshizawa et al. (1993) showed that the memory capacity is theoretically $0.4N$ when the parameters are optimally determined. Shiino and Fukai (1993) applied their theory based on the signal-to-noise analysis to a variant model with a nonmonotonic output function, and obtained a similar result for the memory capacity of $0.42N$. Moreover, Yoshizawa et al. (1993) suggested that it seems that there are no spurious memories, and the network becomes chaotic when it fails to make a proper association, namely, the "I don't

know” state. It should be noted that in all of the studies above, memories have been represented as fixed-point attractors of the dynamical systems, while memories are physiologically attributed to dynamical activities.

On the other hand, recently, many associative memory systems based on nonequilibrium dynamical systems have been proposed (Nara et al., 1993; Hayashi, 1994). Among them, we have previously proposed an associative memory system (Ishii et al., 1996) based on Kaneko’s GCM. In our system, each memory is represented as a spatially coherent oscillation, and the learning rule is of the autocorrelational type. However, in our system, both the memory capacity and the basin volume for each memory are larger than in the Hopfield model employing the same learning rule. This result implies that the chaotic dynamics employed in our system is more efficient than the relaxation dynamics employed in the Hopfield model. Nevertheless, even in our system, spurious memories (Gardner, 1986), i.e., the system’s equilibria that do not correspond to any of the proper memories, exist, which inhibit the system from having a larger memory capacity and larger basin volumes.

The system will be improved if we employ a better learning or coding scheme such as the generalized-inverse matrix method (Kohonen, 1977; Kanter & Sompolinsky, 1987), sparse coding (Palm, 1980; Amari, 1989), mean field theory learning (Peterson & Hartman, 1989), or another. In this paper, however, we aim to reduce spurious memories in our associative memory system by modifying its dynamics. In our new system, spurious memories are noticeably reduced, thereby resulting in a larger memory capacity than the original system. Our research is inspired by the study of nonmonotonic output functions (Morita, 1993; Yoshizawa et al., 1993; Shiino & Fukai, 1993). In this paper, we experimentally compare our new system with a variant system with a nonmonotonic output function. We also give an interpretation as to why such an improvement can be achieved in our new system.

This paper is organized as follows. In Section 2, we introduce our previous associative memory system based on GCM, and a model with a nonmonotonic output function. In Section 3, we propose the new system. The behavior of the new system is described in Section 4. In Section 5, we experimentally evaluate the new system. In Section 6, we discuss the reason why such an improvement can be achieved in the new system. Section 7 sums up the paper.

2 Associative memory systems

An associative memory is an information-processing problem that is described as (Hertz et al., 1991) “storing a set of patterns in such a way that when presented with a new pattern, the network responds by producing whichever one of the stored patterns most closely resembles the new pattern.”

Let $\{\xi^1, \xi^2, \dots, \xi^p \mid \xi^k \in \{1, -1\}^N\}$ be a set of N -dimensional binary patterns (memories) to be stored. ξ_i^k denotes the i th element value in the k th binary pattern and p is the number of stored patterns. The binary patterns are randomly prepared, namely, the probability of $\xi_i^k = 1$ is 0.5. Here, we prepare an autocorrelation matrix of the set of patterns:

$$J_{ij} = \frac{1}{N} \sum_{k=1}^p \xi_i^k \xi_j^k. \quad (1)$$

$J_{ii} = 0$ for all i . In this paper, we study dynamical systems employing the autocorrelational learning rule (1), i.e., Hebbian learning.

Memory capacity means the largest number of memories that can be stored in a system. p/N is called the storage rate. In order to see the behavior of a system, let us define the overlap at time t as:

$$m(t) = \frac{1}{N} \sum_{i=1}^N O_i(t) \xi_i, \quad (2)$$

where ξ is the target memory and $O(t)$ is the system's output at time t . When the overlap is equal to 1, the system's output is equal to the target. When the overlap is around 0, the system's output has no correlation with the target.

2.1 Associative memory based on GCM

We previously proposed a modified GCM model called "S-GCM" (Ishii et al., 1996), which is designed for information-processing applications, e.g., associative memory. Our S-GCM employs a cubic map called an S-MAP instead of the logistic map employed in the original GCM. This modification makes it easy for each unit to represent one bit, i.e., -1 or 1 . Our S-GCM has attractors called "cluster frozen attractors" over a wide range of its parameters. Therefore, our S-GCM can represent binary spatial patterns as its attractors. In this section, we introduce our basic associative memory system based on S-GCM (Ishii et al., 1996).

Our basic model is given by

[System \mathcal{CF}]

$$x_i(t+1) = (1 - \epsilon) f_i(x_i(t)) + \frac{\epsilon}{N} \sum_{j=1}^N f_j(x_j(t)) \quad (3a)$$

$$f_i(x) = f(x; \alpha_i) = \alpha_i x^3 - \alpha_i x + x \quad x \in [-1, 1], \quad (3b)$$

where $x_i(t)$ denotes the i th unit's value at time t , N is the number of units, and t denotes the discrete-time. ϵ is a constant parameter. The main part of each unit's dynamics is given by the cubic function S-MAP (3b). The remaining portion, i.e., a summation part in (3a), is defined as feedback from the "mean-field." The S-MAP f has a bifurcation parameter α , and it produces chaos with a specific value of α . Its function shape and the bifurcation diagram over the bifurcation parameter α are shown in Figures 1(a) and 1(b), respectively. Due to the symmetric function shape of the S-MAP, two-cycle periodicity is likely to be dominant in each unit's motion in \mathcal{CF} ; namely, an element tends to take positive values and negative values alternately. Such two-cycle periodicity can be regarded as a binary representation by distinguishing the two phases, as will be shown below.

In order to use \mathcal{CF} as an associative memory system, let us define the input and output methods. First, we define a function V that converts a binary vector $\mathbf{I} \in \{-1, 1\}^N$ to a continuous state vector $\mathbf{V}(\mathbf{I}) \in [-1, 1]^N$ as:

$$V(\mathbf{I})_i = \begin{cases} x^+ + rand & \text{if } I_i = 1 \\ x^- + rand & \text{if } I_i = -1 \end{cases}, \quad (4)$$

where x^+ and x^- are two-cycle periodic solutions of the S-MAP with $\alpha = \alpha_{min}$ ($= 3.4$), namely, $f(x^+) = x^-$ and $f(x^-) = x^+$ ($x^+ > 0 > x^-$). $rand$ is a small random value. In order

to input an N -dimensional binary vector \mathbf{I} to \mathcal{CF} , the initial state is set as $\mathbf{x}(0) = \mathbf{V}(\mathbf{I})$. In order to get an output $\mathbf{O}(t)$ from \mathcal{CF} at time t , we just apply the sign function to $\mathbf{x}(t)$, namely, $\mathbf{O}(t) = \text{sgn}(\mathbf{x}(t))$, where $\text{sgn}(x) = 1$ (-1) if $x \geq 0$ (< 0). Since two-cycle periodicity is dominant in \mathcal{CF} , the binary output at time $t + 1$ is often identical to the reverse of the output at time t , i.e., $\mathbf{O}(t + 1) = -\mathbf{O}(t)$. In the following, an output of \mathcal{CF} is observed at an even time step. Therefore, our output method assigns 1 and -1 to each phase of the dominant two-cycle periodicity.

Since α is the bifurcation parameter of the S-MAP, we say that when α_i is large, the i th element is chaotic, and when α_i is small, the element is stable. In our system, the evolution of α_i in (3) is defined as follows:

$$\alpha'_i = \alpha_i + (\alpha_i - \alpha_{min}) \tanh(-\beta x_i u'_i) \quad (5a)$$

$$u'_i = \sum_{j=1}^N J_{ij} x_j, \quad (5b)$$

where α_{min} and β are constant parameters. In (5a), α_i is additionally controlled so as not to exceed $\alpha_{max} = 4.0$. Parameters are set at $\epsilon = 0.1$, $\alpha_{min} = 3.4$, and $\beta = 0.2$. The parameter control (5) is done once every four time steps, i.e., at $t = 4, 8, 12, \dots$, in order to suppress the effect of small perturbations in the system. In this sense, the control (5) is described without using t . In \mathcal{CF} , \mathbf{x} and \mathbf{u} are called the system's state and the system's internal potential, respectively.

Let us see the behaviors of \mathcal{CF} . Figure 2 shows the time-series of the overlap (2), when the input \mathbf{I} is given so that the initial overlap $m(0)$ is set at various specific values. Figures 2(a) and 2(b) show $p = 0.125N$ and $p = 0.250N$, respectively. When the number of stored patterns is relatively small, i.e., $0.125N$, \mathcal{CF} can recall a target pattern if the initial overlap is large. However, the basin of attraction disappears when the number of stored patterns is large, i.e., $0.250N$.

Figures 2(a) and 2(b) imply that the memory capacity of \mathcal{CF} is larger than $0.125N$ but smaller than $0.250N$. According to our experiments, the memory capacity of \mathcal{CF} is estimated at $0.186N$ (Ishii et al., 1996), which is about 50% larger than that of the Hopfield model. Furthermore, \mathcal{CF} has a larger basin volume for each stored pattern than the Hopfield model, unless the target pattern is very biased (Ishii et al., 1996).

Figure 3 shows an example association process. $N = 100$, $p = 10$, the initial overlap $m(0) = 0.6$, and the association was successful. In Figure 3(a), highly chaotic motions are observed at the early association stage. As time elapses, these motions become quiet, and the association is completed successfully when the system falls into a 4-cluster frozen attractor. Since Figure 3(a) shows the time-series for every four time steps, the above-mentioned dominant two-cycle periodicity cannot be observed. Figure 3(b) shows the time-series of the overlap $m(t)$ during this association process.

2.2 Nonmonotonic output function

Next, we introduce a differential equation system with a nonmonotonic output function (Morita, 1993). Here, we adopt an end-cut-off type function as a nonmonotonic output function, which has been used by Shiino and Fukai (1993). The model is defined as

[System NM]

$$\dot{u}_i = -u_i + \sum_{j=1}^N J_{ij} F(u_j) \quad (6a)$$

$$F(u) = \begin{cases} \text{sgn}(u) & \text{if } |u| < \theta \\ 0 & \text{if } |u| \geq \theta \end{cases}, \quad (6b)$$

where \dot{u}_i denotes the time derivative of u_i , with respect to the continuous-time t . A system's output at time t , $\mathbf{O}(t)$, is $\text{sgn}(\mathbf{u}(t))$. $\mathbf{x} \equiv F(\mathbf{u})$ and \mathbf{u} are called the system's state and the system's internal potential, respectively, although the state of the system can be described only by \mathbf{u} .

Shiino and Fukai applied their theory based on the signal-to-noise analysis to a model (6), and obtained the maximum memory capacity of $0.42N$ for $\theta \approx 0.7$. This result was also experimentally confirmed in their paper, and the capacity value with the end-cut-off type output function was found to be larger than Morita's experimental result (Morita, 1993), $0.32N$, and a theoretical estimation by Yoshizawa et al. (1993), $0.4N$. This variance in the memory capacity values stems from the difference of the nonmonotonic function shapes.

Next, let us take a look at the behavior of NM. Figures 4(a) and 4(b) show the time-series of the overlap (2), when the initial overlap $m(0)$ is set at various values. The parameter θ was set at 0.7, and each initial internal potential was set at $\mathbf{u} = 0.6\mathbf{I}$, where \mathbf{I} is the input binary pattern. Figures 4(a) and 4(b) show $p = 0.25N$ and $p = 0.50N$, respectively. When the number of stored patterns is relatively small, i.e., $0.25N$, NM can recall a target pattern from a fairly distant initial state. However, the basin of attraction disappears when the number of stored patterns is large, i.e., $0.50N$.

In Figure 4(a), we can see that when the system cannot recall the target pattern, the system's behavior continues to be unstable. This feature is very important for an associative memory system. In the conventional Hopfield model, since the autocorrelation matrix (1) is a condensed representation of the stored patterns, there is no way to know whether the obtained association result is successful or unsuccessful, i.e., a proper memory or a spurious memory. With the nonmonotonic output function, however, we can know when the obtained result is unsuccessful because unstable motions remain in such a case (Morita, 1993; Yoshizawa et al., 1993). There is another important feature in NM. When the system can recall a target pattern, it seems that there is no discrepancy between the system's output and the target pattern, even if the system is near memory saturation (Yoshizawa et al., 1993). Although this feature is theoretically ensured only when the storage rate is relatively small (Shiino & Fukai, 1993), our experiments show that there is almost no discrepancy even when the storage rate is large. Namely, the system can recall the complete pattern of a target. It is known that in the Hopfield model there is a discrepancy between the output and the target, when the system is near memory saturation (Amit et al., 1985b; Hertz et al., 1991).

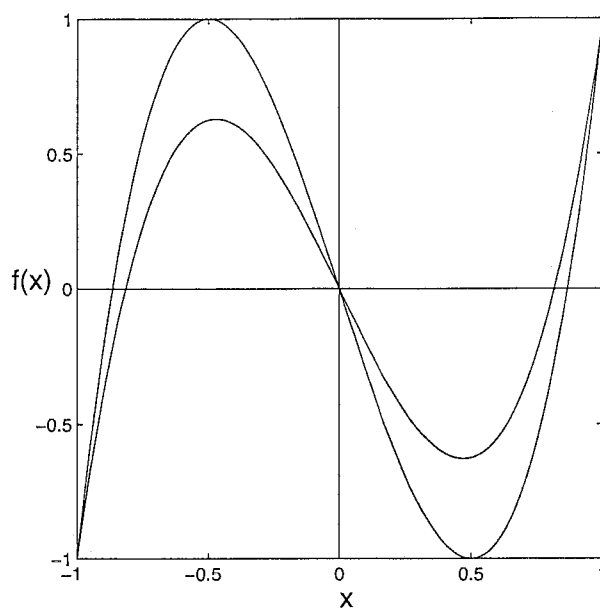


Figure 1(a)

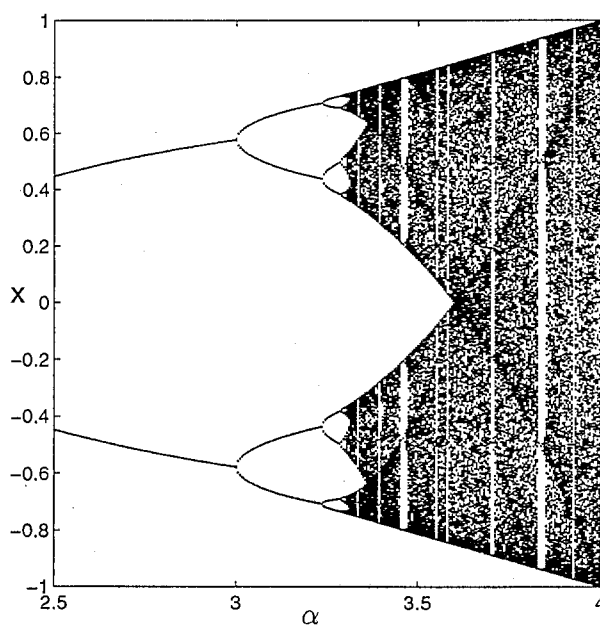


Figure 1(b)

(a) A cubic function S-MAP, $f(x) = \alpha x^3 - \alpha x + x$, where $\alpha = 3.0$ and $\alpha = 4.0$. (b) Bifurcation diagram of the S-MAP ($2.5 \leq \alpha \leq 4.0$).

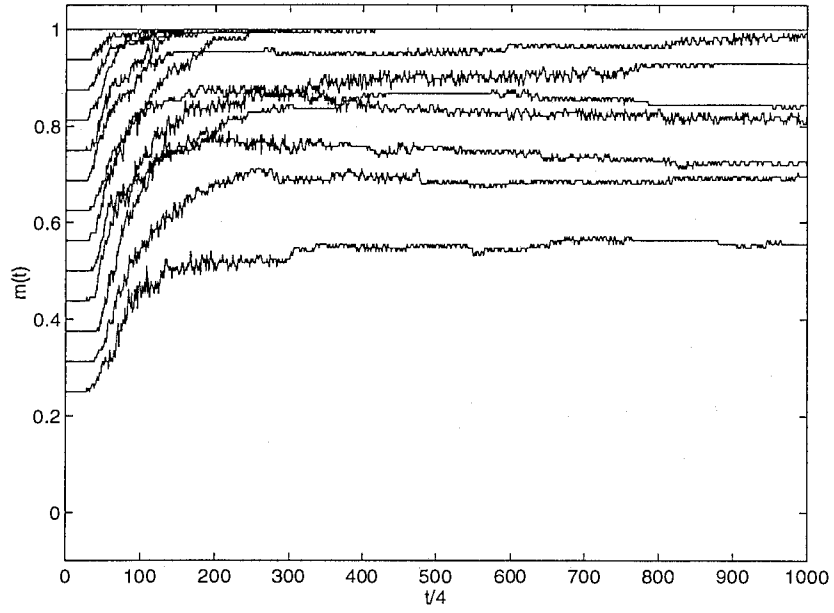


Figure 2(a)

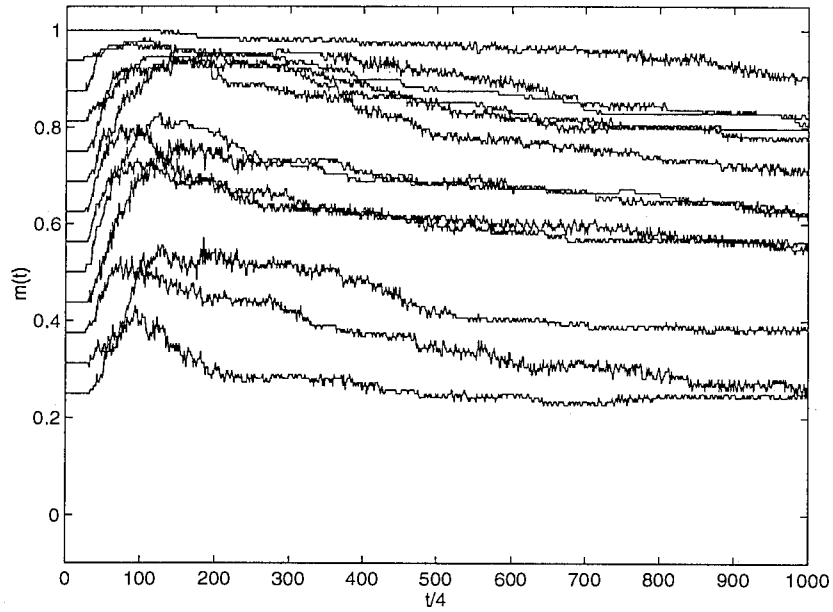


Figure 2(b)

Time-series of the overlap $m(t)$ in \mathcal{CF} . Parameters are set at: $\alpha_{min} = 3.4$, $\epsilon = 0.1$, and $\beta = 0.2$. Initial values of α_i are set at 3.5 for every i . The abscissa denotes the time ($t = 4, 8, 12, \dots, 4 \times 1000$). $N = 256$. (a) $p = 32 = 0.125N$. (b) $p = 64 = 0.250N$.

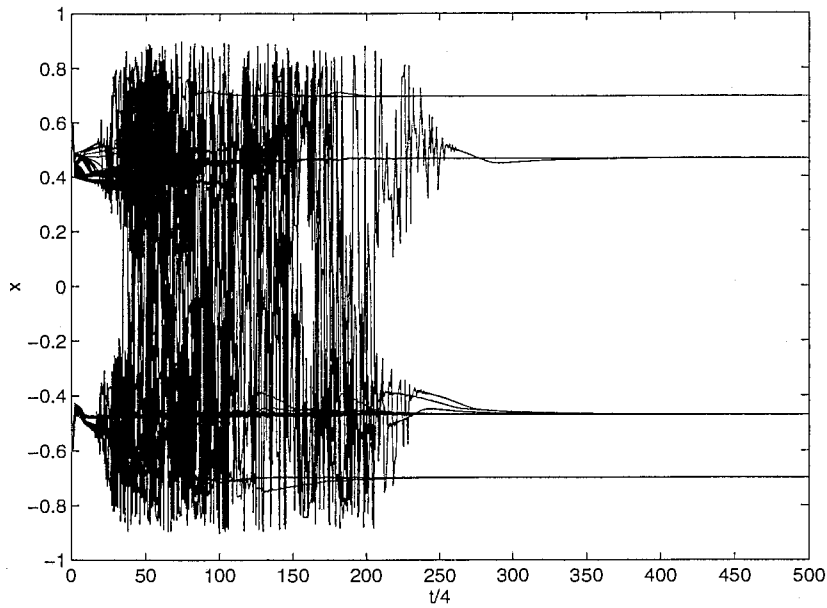


Figure 3(a)

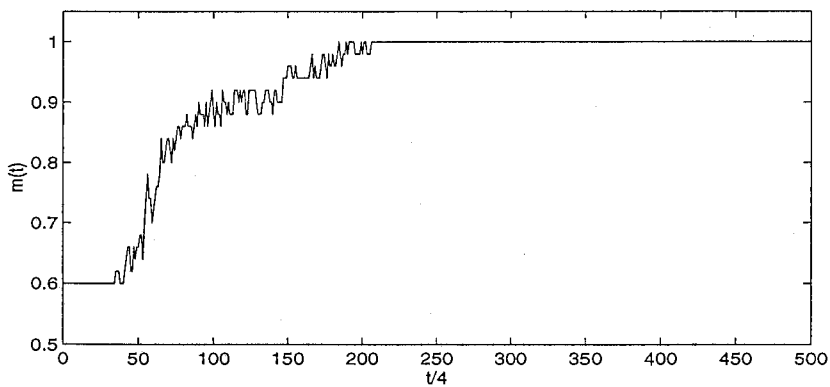


Figure 3(b)

An example association process of \mathcal{CF} . $N = 100, p = 10$, the initial overlap $m(0) = 0.6$, and the association was successful. (a) Time-series of all the units are plotted every four time steps. The abscissa denotes the time ($t = 4, 8, 12, \dots, 4 \times 500$). (b) Time-series of the overlap $m(t)$.

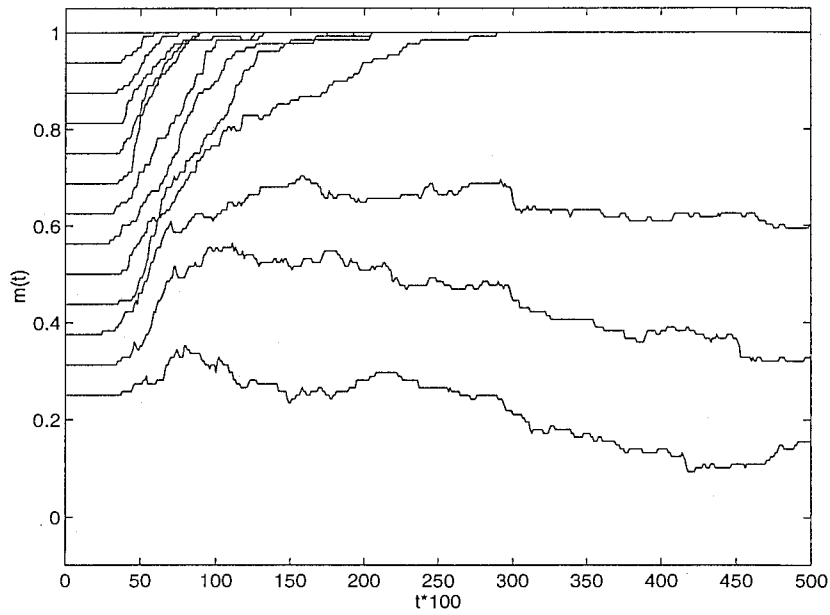


Figure 4(a)

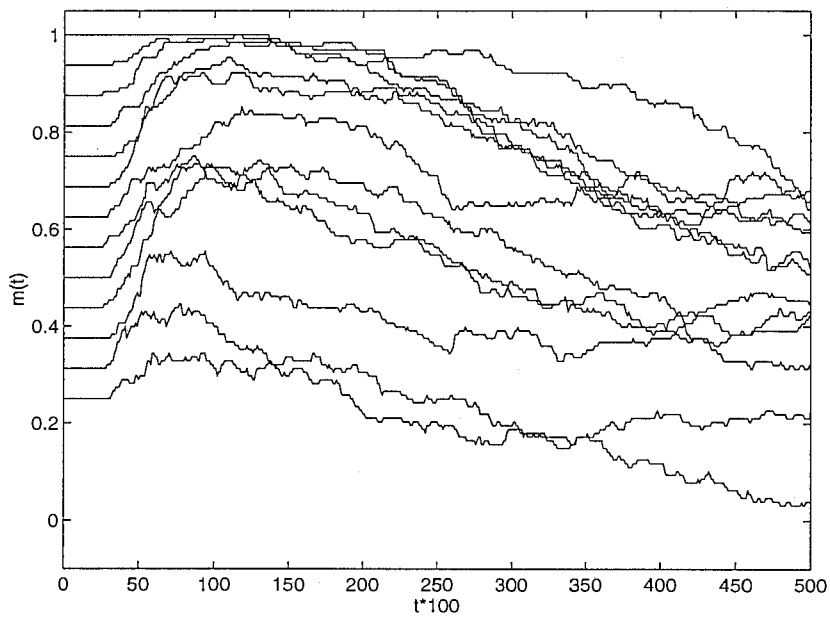


Figure 4(b)

Time-series of the overlap $m(t)$ in NM, where $N = 256$ and $\theta = 0.7$. The differential equation (6) was calculated by the Euler method with the time-interval $\delta t = 0.01$, and the initial internal state was set at $\mathbf{u}(0) = 0.6\mathbf{I}$, where \mathbf{I} is the input binary pattern. The abscissa denotes the continuous-time t . (a) $p = 64 = 0.25N$. (b) $p = 128 = 0.50N$.

3 Model description

The associative memory system \mathcal{CF} introduced in Section 2.1 has a better ability than the Hopfield model, although our system and the Hopfield model employ the same autocorrelational learning scheme (1). The reason is considered to be as follows. In \mathcal{CF} , with its chaotic dynamics in the early association stage, the system state can escape from spurious memory states. On the other hand, since the Hopfield model employs a gradient-descent dynamics that minimizes its Lyapunov function, it cannot escape from the spurious minimum of the Lyapunov function. Nevertheless, even in \mathcal{CF} , spurious memories exist, which inhibit the system from having a larger memory capacity or larger basin volumes.

In order to deal with the problem, we propose a new associative memory system.

[System PCCE]

$$x_i(t+1) = f(x_i(t); \alpha_i(t)) \quad (7a)$$

$$f(x; \alpha) = \alpha x^3 - \alpha x + x. \quad (7b)$$

Like in \mathcal{CF} , $x_i(t)$ denotes the i th unit's value at discrete-time t , and f is the S-MAP. The proposed model (7) is an ensemble of chaotic elements that are primarily independent of each other but dependent through the bifurcation parameter α . In \mathcal{CF} , each element is dependent on the others in its value through homogeneous couplings. However, in the proposed model, we discard the direct couplings. This reason will be described below. The evolution of α_i is defined as follows:

$$\alpha'_i = \alpha_{mid} + (\alpha_{mid} - \alpha_{min}) \tanh(-\beta x_i u'_i) \quad (8a)$$

$$u'_i = (1 - \kappa)u_i + \kappa \sum_{j=1}^N J_{ij} g(\alpha_j) x_j \quad (8b)$$

$$g(\alpha) = \begin{cases} 1 & \text{if } \alpha > \alpha_u \\ 0 & \text{if } \alpha < \alpha_l \\ (\alpha - \alpha_l)/(\alpha_u - \alpha_l) & \text{otherwise} \end{cases}, \quad (8c)$$

where α_{mid} , α_{min} , β , κ , α_l , and α_u are constant parameters that satisfy $\alpha_{min} < \alpha_l \leq \alpha_u < \alpha_{max} = 4.0$, $\alpha_{min} < \alpha_{mid} < \alpha_{max}$, $\beta > 0$, and $0 < \kappa \ll 1$. Each α_i is additionally controlled so as not to be larger than α_{max} . The evolution (8) is done once every 4 time steps, i.e., at $t = 4, 8, 12, \dots$. In this sense, the evolution is described without using t . In the following, we call the dynamical system, (7) and (8), Parametrically Coupled Chaotic Elements (PCCE).

In order to use PCCE as an associative memory system, let us define the input and output methods. To input a binary pattern \mathbf{I} to PCCE, we set $\mathbf{u}(0) = \mathbf{I}$ and $\mathbf{x}(0) = V(\mathbf{I})$, where V is defined by (4). A system's output at time t , $\mathbf{O}(t)$, is given by $\text{sgn}(\mathbf{x}(t))$. \mathbf{x} and \mathbf{u} are called the system's state and the system's internal potential, respectively. $\mathbf{y} \equiv g(\alpha)\mathbf{x}$ is called the system's effective state. In the following experiments, the system parameters are set at: $\alpha_{mid} = 3.5$, $\alpha_{min} = 3.1$, $\alpha_l = 3.4$, $\alpha_u = 3.5$, $\beta = 2.0$, and $\kappa = 0.05$.

Let us discuss the meaning of the new parameter control method (8). (8a) has a similar role to (5a). If the term $(-x_i u'_i)$, which is called the i th partial energy, is large and positive, α_i becomes large, and if the i th partial energy is small and negative, α_i becomes small. β is the parameter that determines the sharpness of this control. Next, in order to see the

difference between (5b) and (8b), let us consider a case where $g(\alpha_i) = 1$ for every i , for a while. In this case, (8b) is a Euler difference equation of the differential equation:

$$\dot{u}_i = -u_i + \sum_{j=1}^N J_{ij}x_j, \quad (9)$$

which is identical to the definition of the Hopfield model's internal potential. (5b) corresponds to the MFT version of (9). At an equilibrium state of PCCE with $g(\alpha_i) = 1$, (8b) is almost equivalent to (5b). Since PCCE never equilibrates, however, (5b) and (8b) differ in their stability. Although the system does not equilibrate, since $(-\sum_i x_i u'_i)$ at an equilibrium state has the same functional form as the conventional energy function, the term $(-x_i u'_i)$ is called the i th partial energy in PCCE.

The most important modification is the existence of $g(\alpha)$ (8c), which is called the gain function (Ishii, 1994). Figure 5 shows the function shape of the gain function. As this figure shows, the gain is 1 for a relatively large α value, i.e., when the unit's state is chaotic, while the gain is 0 for a relatively small α value, i.e., when the unit's state is stable. The meaning of this gain function will be discussed in Section 6.

In \mathcal{CF} , each element is dependent on the others through homogeneous couplings. Such direct couplings are important in the system, because with the control method (5a) the system falls into a cluster frozen attractor (see Figure 3(a)), which is regarded as a successful association result. However, with the control method (8a) the system does not equilibrate at a cluster frozen attractor, because the parameter α_i varies one by one. Figure 6 shows an example association process of PCCE. According to our preliminary experiments, if we add homogeneous couplings to PCCE, its memory capacity expands a little. However, since the role of the couplings is not clear in PCCE, we discard the couplings in order to simplify the model definition in this paper.

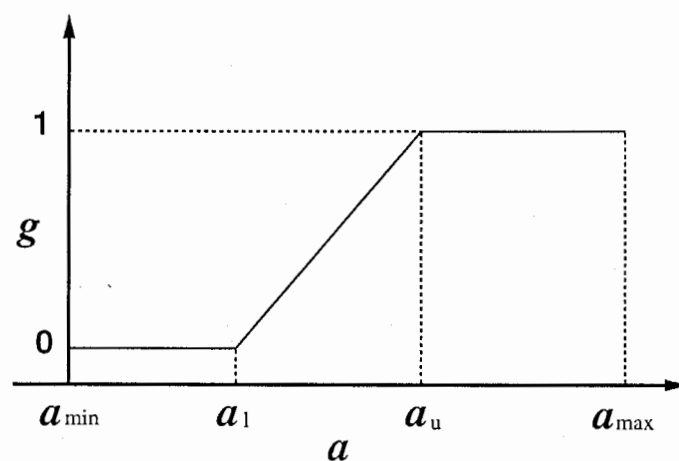


Figure 5

Function shape of the gain function g .

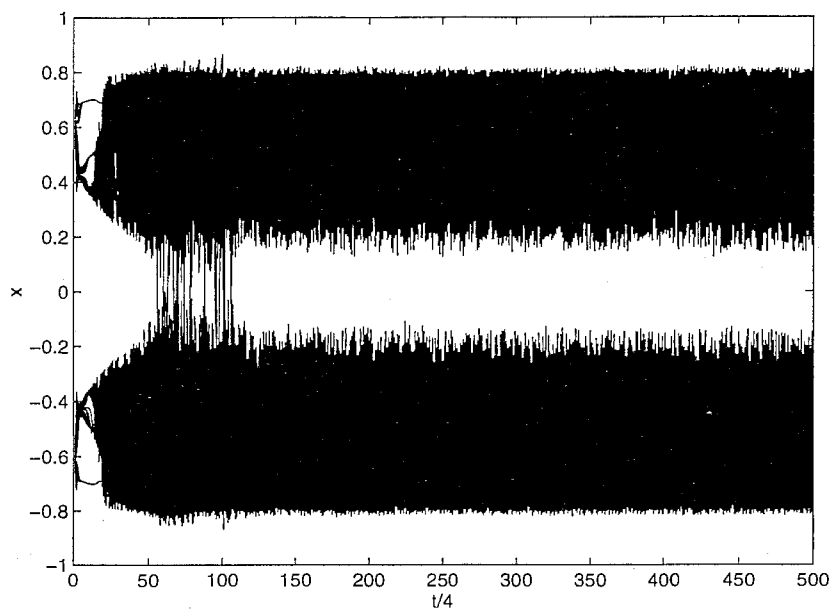


Figure 6(a)

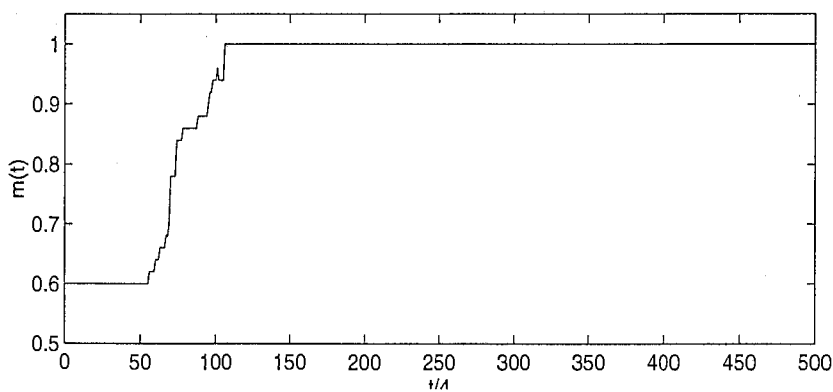


Figure 6(b)

An example association process of PCCE. $N = 100, p = 40$, the initial overlap $m(0) = 0.6$, and the association was successful. (a) Time-series of all the units are plotted every four time steps. The abscissa denotes the time ($t = 4, 8, 12, \dots, 4 \times 500$). (b) Time-series of the overlap $m(t)$.

4 System behavior

Figure 7 shows the time-series of the overlap $m(t)$ of PCCE, when the input is given so that the initial overlap $m(0)$ is set at various values. Figures 7(a), 7(b), and 7(c) show $p = 0.25N$, $p = 0.50N$, and $p = 0.75N$, respectively. As Figure 7(a) shows, when the number of stored patterns is relatively small, i.e., $p = 0.25N$, the system can recall the target from an input that is distant from the target. When the number of stored patterns is relatively large, i.e., $p = 0.50N$, the basin of attraction becomes small as Figure 7(b) shows. In this case, if the input is close to the target, the system can recall the target, while if the input is far from the target, the system fails to make the association. When the number of stored patterns is very large, i.e., $p = 0.75N$, even if the input is set at the target pattern itself, the state becomes distant from it as time elapses as Figure 7(c) shows. This means that the system cannot store so many patterns.

Figure 7(b) shows that the memory capacity of PCCE is larger than $0.5N$, which is much larger than those of the Hopfield model ($0.138N$) and our previous model \mathcal{CF} ($0.186N$). It is also larger than those of the differential equation models with nonmonotonic output functions ($0.32N \sim 0.42N$).

Let us now look at the microscopic behavior of a PCCE association process. In the experiment, $N = 256$, $p = 0.5N = 128$, initial overlap $m(0) = 0.5$, and the association was successful. Figures 8(a), 8(b), and 8(c) show the time-series of x_1 , u_1 , and α_1 , respectively. These figures show that the first element did not change its output during the process. Figures 9(a), 9(b), and 9(c) show the time-series of x_2 , u_2 , and α_2 , respectively. These figures show that the second element changed its output from 1 to -1 . It should be noted that in both the first and second element's states, two-cycle periodicity is dominant like in \mathcal{CF} , which is not seen in Figures 8(a) and 9(a), because both figures show the time-series for once in every four time steps. In Figure 8, the internal potential u_1 continues to be positive, and the bifurcation parameter α_1 remains small so as not to exceed the band-merge point of the S-MAP (see Figure 1(b)). The element's state then preserves the input's sign, as Figure 8(a) shows. In contrast, in the case of Figure 9, the internal potential u_2 changes its value from positive to negative as time elapses. This causes a temporal increase of the bifurcation parameter α_2 so as to exceed the band-merge point of the S-MAP. The element's state then no longer preserves the input's sign and x_2 turns negative as Figure 9(a) shows.

Figure 10 shows the time-series of the activation rate, which is given by $(\frac{1}{N} \sum_i g(\alpha_i))$, during this successful association process. After a short transient period of $0 \leq t/4 < 100$, the activation rate becomes almost constant at about 0.45, which means that about 45% of the units affect other units. If we define the activation rate in NM (6) as $(\frac{1}{N} \sum_i |x_i|)$, this rate can be controlled by the parameter θ , because the rate after a target memory is successfully recalled is close to the parameter θ value (Shiino & Fukai, 1993). This can be confirmed when the storage rate (p/N) is almost 0 as follows. An equilibrium state of (6) is given by

$$x_i = F \left(\sum_{j=1}^N J_{ij} x_j \right) = F \left(\sum_{k=1}^p \xi_i^k h^k \right) \quad (i = 1, \dots, N), \quad (10)$$

where $h^k \equiv \frac{1}{N} \sum_j \xi_j^k x_j$ is called the effective overlap with the k th memory ξ^k in NM. Since $p/N \approx 0$, the effect of $J_{ii} = 0$ is ignored in (10). When an equilibrium state \mathbf{x} corresponds

to the target ξ^1 , h^k ($k > 1$) can be neglected compared with h^1 . In addition, by multiplying both hands of (10) by ξ_i^1/N and summing over i , one can obtain

$$h^1 = F(h^1). \quad (11)$$

If the discontinuous function F (6b) is replaced by the continuous function:

$$F_\delta(u) = \begin{cases} \text{sgn}(u) & \text{if } |u| < (\theta - \delta) \\ (\text{sgn}(u)\theta - u)/\delta & \text{if } (\theta - \delta) \leq |u| < \theta \\ 0 & \text{if } |u| \geq \theta \end{cases}, \quad (12)$$

equation (11) has a solution: $h^1 \approx \theta$ for $\theta < 1$. Here, $0 < \delta \ll \theta$. Since the function F (6b) is given as the limit $\delta \rightarrow +0$ of F_δ (12), h^1 becomes close to θ and it sticks to that value as the differential equation (6) converges. Further explanation of $h^1 \approx \theta$ is given in (Shiino & Fukai, 1993). From $h^1 = \theta$, we know that the activation rate becomes θ . However, since NM often oscillates with $\theta = 0.45$ even if it starts from the target memory, it is difficult in NM (6) to reduce the activation rate to 45%.

The activation rate is relevant to the stability of a successful retrieval state. When a retrieval state corresponding to a target memory is highly correlated with the non-target memories, the retrieval state becomes unstable. This situation actually occurs in the Hopfield model with a larger number of memories than the capacity value. If we can make the activation rate low so that the retrieval state has a small correlation with the non-target memories, the memory capacity will increase, like that achieved in the generalized-inverse matrix method (Kohonen, 1977; Kanter & Sompolinsky, 1987). The activation rate can be made fairly small in PCCE, which prevents a successful retrieval state from being disturbed by the noise from non-target memories so as to make the retrieval state stable.

In order to see further, let us define several order parameters. Equation (8a) means that if x_i and u_i' have opposite signs, the i th element is disturbed so that x_i and u_i' take the same sign. In (8b), u_i' is altered by the term $\sum_i J_{ij}g(\alpha_i)x_i \equiv \sum_i J_{ij}y_i$, which can be decomposed as

$$\begin{aligned} \sum_{j=1}^N J_{ij}y_j &= \xi_i^1 \left(\frac{1}{N} \sum_{j=1}^N \xi_j^1 y_j \right) + \frac{1}{N} \sum_{k=2}^p \sum_{j=1}^N \xi_i^k \xi_j^k y_j - \frac{p}{N} x_i \\ &= \xi_i^1 h^1 + \sum_{k=2}^p \xi_i^k h^k - \frac{p}{N} x_i, \end{aligned} \quad (13)$$

where ξ^1 is the target pattern, and $h^k \equiv \frac{1}{N} \sum_i \xi_i^k y_i$ is called the effective overlap with the k th memory ξ^k in PCCE. The term h^1 is called the signal term. The second term of (13) is called the crosstalk noise term. The third term corresponds to the zero diagonal elements of the autocorrelation matrix (1), $J_{ii} = 0$. The signal term works to give each u_i the correct sign, while the crosstalk noise term disturbs it. To see the effect of the crosstalk noise term, a variance of the crosstalk noise is defined as (Coolen & Sherrington, 1993)

$$r(t) \equiv \frac{N}{p} \sum_{k=2}^p (h^k)^2. \quad (14)$$

A signal term and a crosstalk variance can be defined for \mathcal{CF} or NM, with the definition $h^k \equiv \frac{1}{N} \sum_i \xi_i^k x_i$. Then, \mathbf{x} is also called the effective state in \mathcal{CF} and NM.

Figures 11(b), 11(c), and 11(d) show the association processes of \mathcal{CF} , NM, and PCCE, respectively, in a two-dimensional phase space of the signal term and the crosstalk variance. For comparison, Figure 11(a) shows a similar figure in the analog Hopfield model with zero temperature, which is defined by (6) with $F = \text{sgn}$. Each figure shows a successful association process starting from an input that is close to the target, $m(0) = 0.75$, and an unsuccessful association process starting from an input that is distant from the target, $m(0) = 0.25$. The Hopfield model stores $0.08N$ memories, \mathcal{CF} stores $0.125N$ memories, NM stores $0.25N$ memories, and PCCE stores $0.5N$ memories. In \mathcal{CF} , when a proper association is done, the signal term becomes large as time elapses. When the association fails, the signal term becomes large temporarily in the early association stage, and then becomes small in the later association stage, while the crosstalk variance increases in the whole association stage. This phenomenon is quite similar to that observed in the Hopfield model, which has been theoretically studied by means of signal-to-noise analysis (Amari & Maginu, 1988; Coolen & Sherrington, 1993; Okada, 1995). In NM, although an association process involves unstable motions, the process in the two-dimensional phase space is qualitatively similar to that of \mathcal{CF} and the Hopfield model. The signal term is smaller than that in \mathcal{CF} and the Hopfield model, due to the low activation rate (≈ 0.7). The crosstalk variance becomes much smaller than that in \mathcal{CF} and the Hopfield model, thereby obtaining a larger memory capacity than the two models. The signal term in PCCE is even smaller than that in NM, due to the low activation rate (≈ 0.45) and the small values of the system's state \mathbf{x} . The crosstalk variance is reduced more significantly than the signal term. Note that at the beginning of a PCCE's association process, the signal term and the crosstalk variance are 0 as Figure 11(d) shows, because the gain of every unit is 0. However, since the input is preserved by the system's state \mathbf{x} and the internal potential \mathbf{u} , the system can make a proper association.

When the crosstalk variance is much smaller than the signal term, the dynamics is considered to be good, because an association process is not disturbed by the crosstalk term. Such good dynamics is implemented in PCCE more significantly than in the other models. When PCCE can recall a target, the crosstalk variance becomes very small, as can be seen in Figure 11(d). This phenomenon can also be observed in NM (see Figure 11(c)). The small crosstalk variance for a successful association process in PCCE implies that the effective state \mathbf{y} is almost uncorrelated with the non-target memories ξ^k ($k = 2, \dots, p$) (see (14)). This will be discussed further in Section 6. In addition, the unstable motions in the early association stage are larger in PCCE than in NM, which is considered to be another reason for the improvement as an associative memory system. It should be noted that when the association is successful, the chaotic motions of PCCE in the later association stage are localized so that the overlap is not disturbed by them.

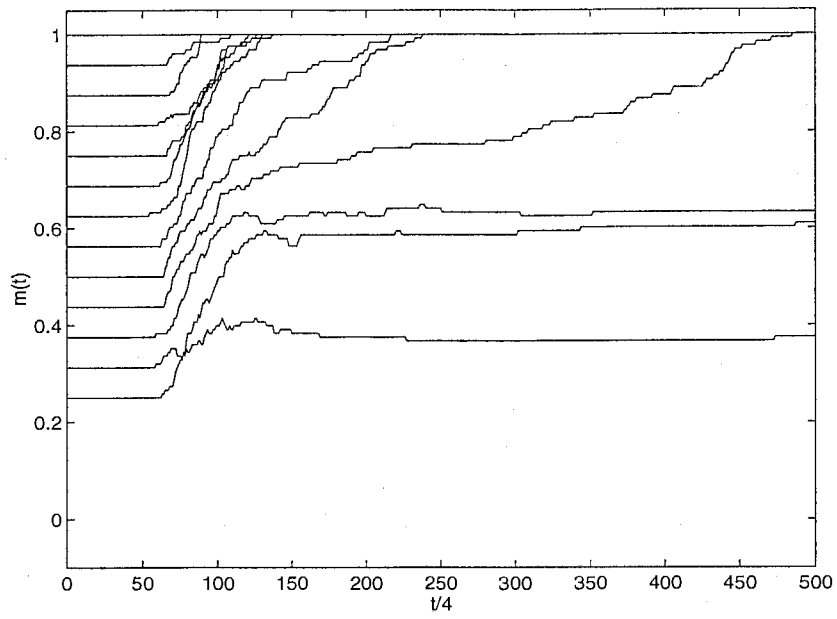


Figure 7(a)

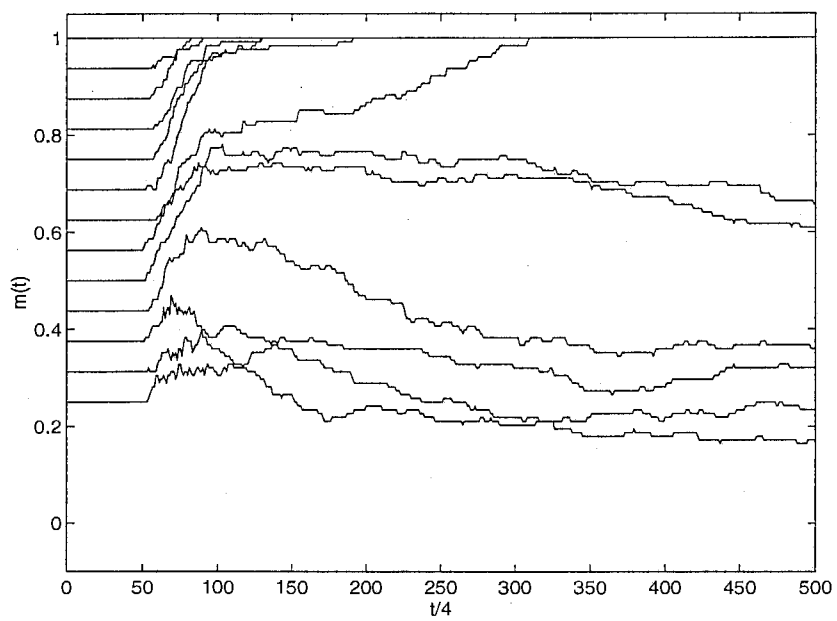


Figure 7(b)

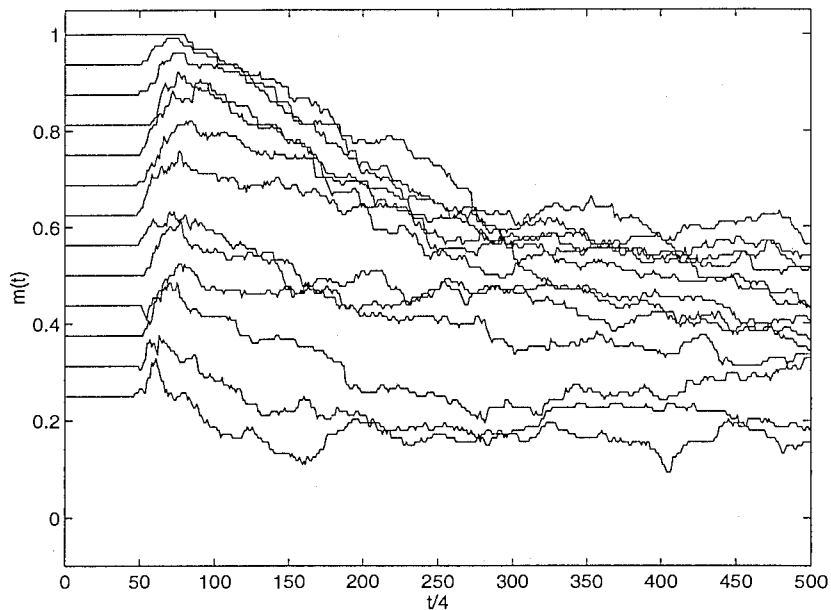


Figure 7(c)

Time-series of the overlap $m(t)$ in PCCE, where $N = 256$. Parameters are set at: $\alpha_{mid} = 3.5, \alpha_{min} = 3.1, \alpha_l = 3.4, \alpha_u = 3.5, \beta = 2.0, \kappa = 0.05$. The abscissa denotes the discrete-time t . (a) $p = 64 = 0.25N$. (b) $p = 128 = 0.50N$. (c) $p = 192 = 0.75N$.

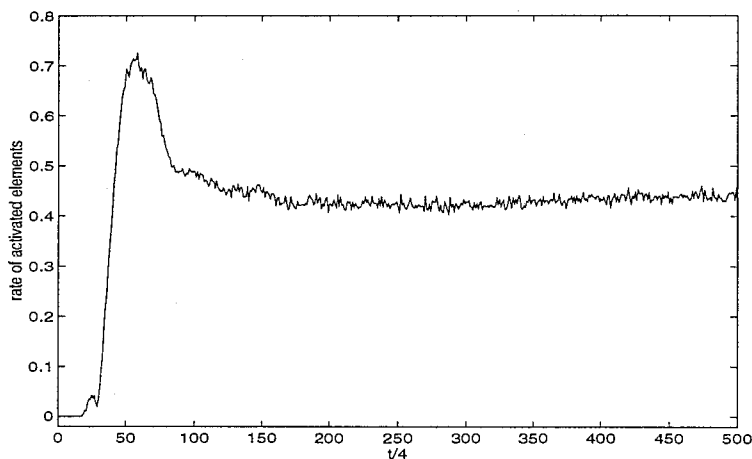


Figure 10

Time-series of the activation rate $(1/N) \sum_i g(\alpha_i)$ during the successful association process shown in Figures 8 and 9.

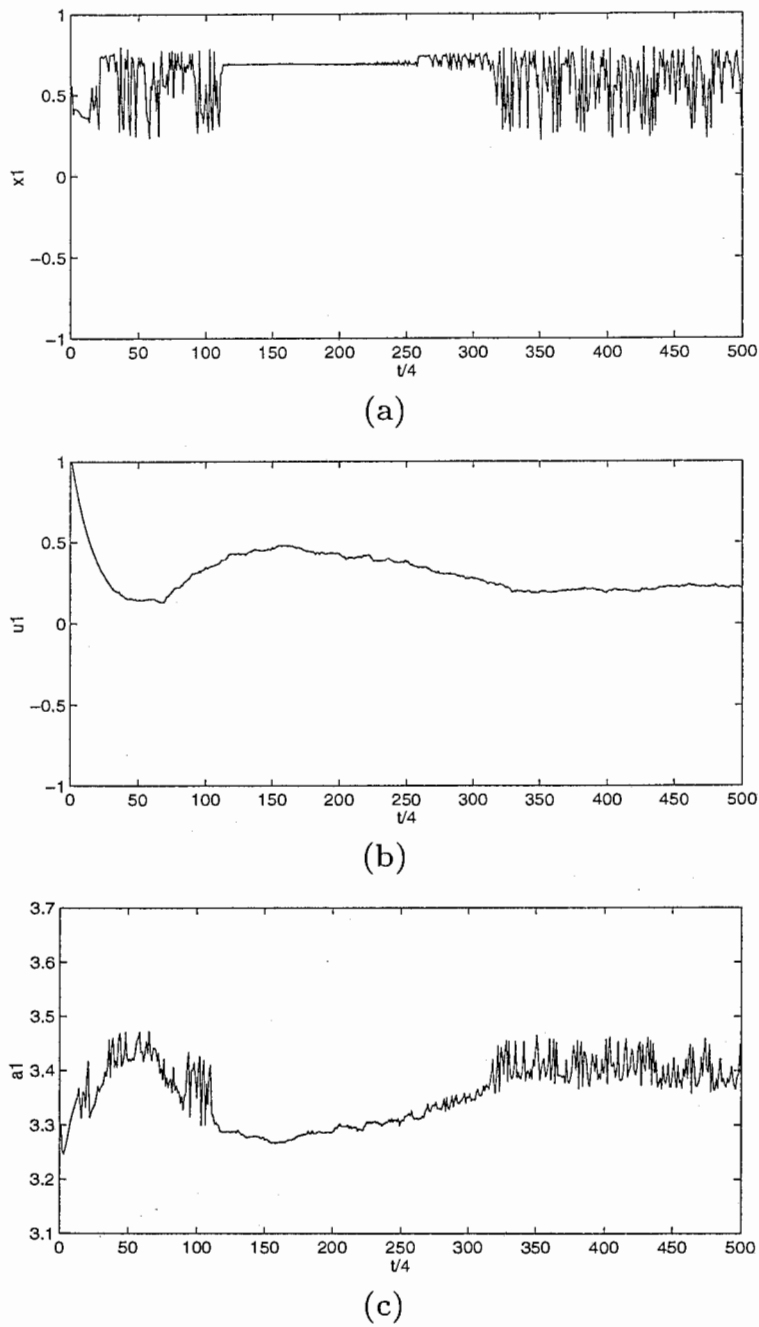
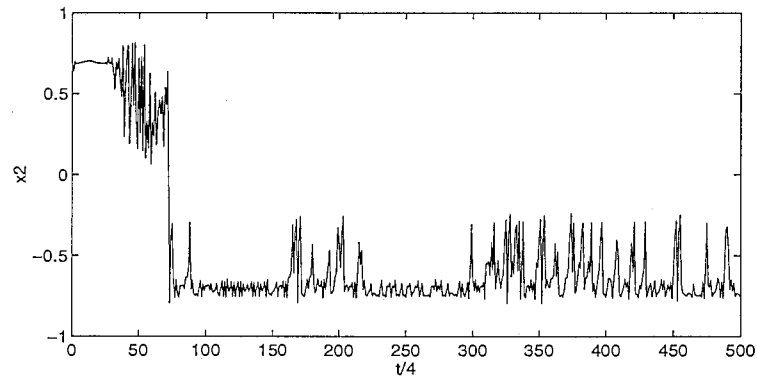
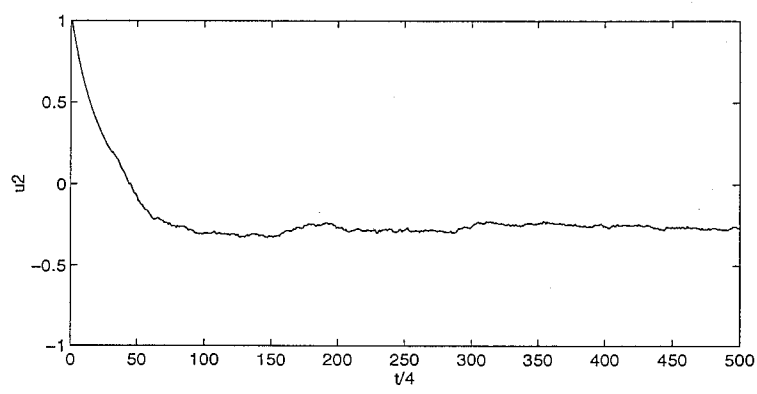


Figure 8

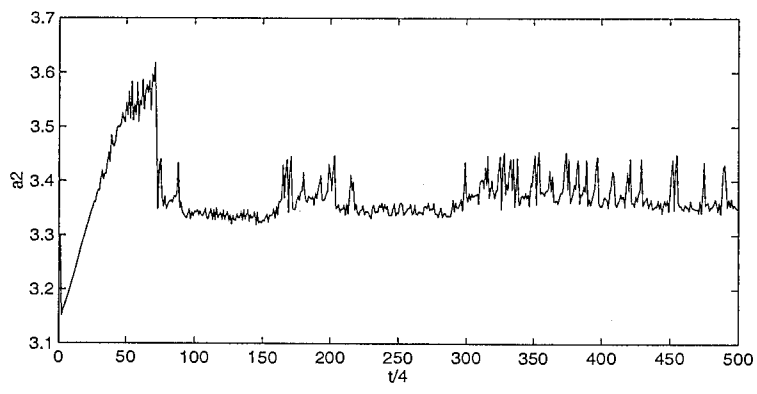
Time-series of the first element that did not change its output during the association process. $N = 256$, $p = 0.5N = 128$, $m(0) = 0.5$, and the association was successful. (a) Time-series of x_1 . (b) Time-series of u_1 . (c) Time-series of α_1 .



(a)



(b)



(c)

Figure 9

Time-series of the second element that changed its output from 1 to -1 during the association process. (a) Time-series of x_2 . (b) Time-series of u_2 . (c) Time-series of α_2 .

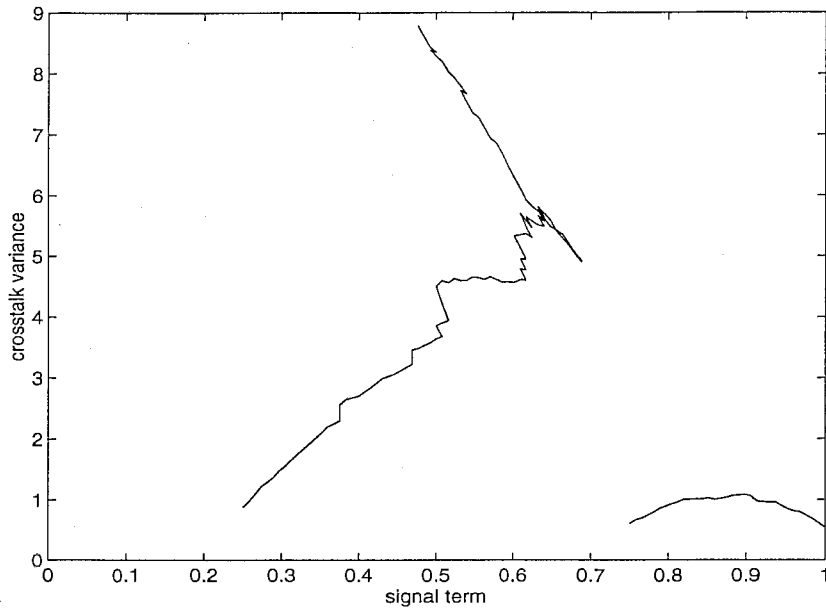


Figure 11(a)

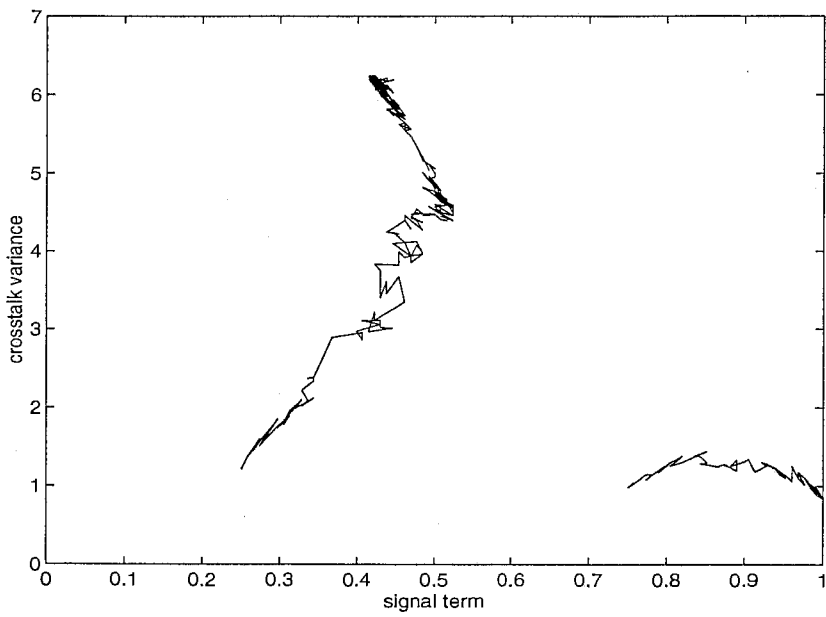


Figure 11(b)

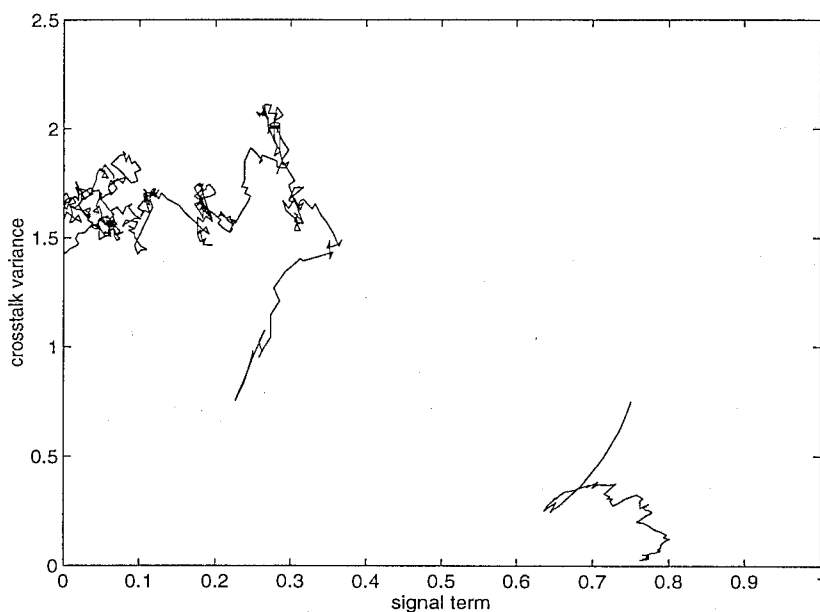


Figure 11(c)

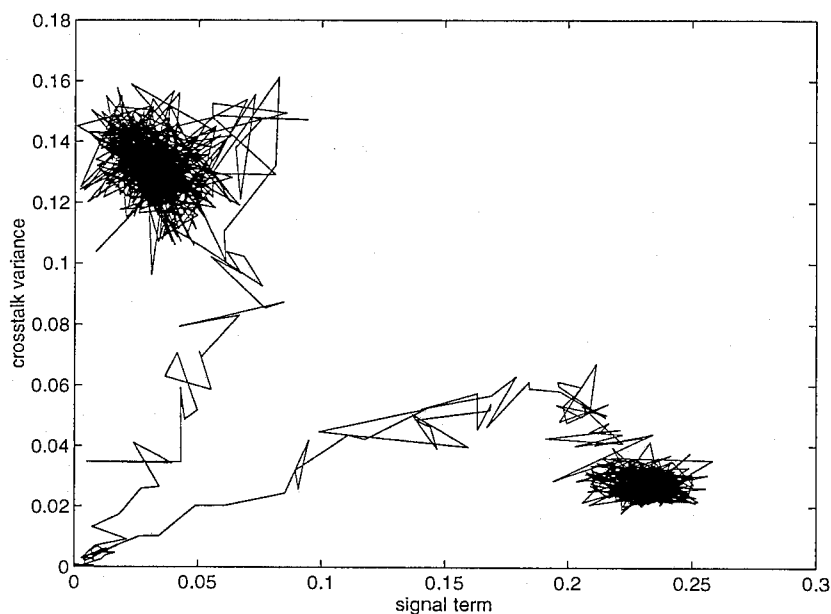


Figure 11(d)

Association processes in a two-dimensional phase space of the signal term and the crosstalk variance. Each figure shows a successful association process starting from an input that is relatively close to the target, $m(0) = 0.75$, and an unsuccessful association process starting from an input that is relatively distant from the target, $m(0) = 0.25$. $N = 256$. (a) The Hopfield model with $0.08N \approx 20$ stored patterns. (b) \mathcal{CF} with $0.125N = 32$ patterns. (c) NM with $0.25N = 64$ patterns. (d) PCCE with $0.5N = 128$ patterns.

5 Evaluation

In this section, the new system PCCE is evaluated as an associative memory system. Here, let us compare PCCE with NM.

Figure 12(a) shows the experimental results of the critical overlap of PCCE for various storage rate (p/N) values. The critical overlap denotes the farthest initial state from the target pattern from which the system can associate the target. The critical overlap also indicates how large the basin of attraction is: the smaller the critical overlap, the larger the basin of attraction. Since the basin of attraction generically has a very complex shape instead of a sphere-like shape, the critical overlap depends on the stored patterns, target pattern, and initial conditions, as well as the storage rate. Therefore, it is estimated as an averaged value. In order to obtain Figure 12(a), we tried to perform association processes 50 times for each storage rate value. The circles and the error bars in Figure 12(a) denote mean values and standard deviations, respectively, for the 50 trials. For comparison, Figure 12(b) shows similar experimental results for NM.

In PCCE, when the system can recall the target, there seems to be no discrepancy between the system's output and the target pattern. Therefore, we can experimentally obtain an "absolute" memory capacity in PCCE. This phenomenon is similar to that in NM (Yoshizawa et al., 1993), although the theory by Shiino and Fukai (1993) shows that the phenomenon is ensured when the storage capacity is fairly small. From Figure 12(a), we can see that PCCE has a large memory capacity, which is estimated as $0.58N$. On the other hand, NM's memory capacity is estimated as $0.39N$ in Figure 12(b), which is a slightly smaller capacity value than the result obtained by Shiino and Fukai (1993). Thus the memory capacity of PCCE is about 50% larger than that of NM and about three times as large as that of \mathcal{CF} . However, PCCE has smaller basins of attraction than NM when the storage rate is small.

The noise from the crosstalk term is small when the storage rate is small, as can be seen in (13). As will be discussed later, PCCE is considered to have a hysteresis mechanism. With a small storage rate, since the disturbance of the noise is too small to beat the hysteresis effect, the association ability is small. However, when the storage rate is not small, the noise from the crosstalk term is large enough to make a proper association, although a storage rate that is too large is also harmful for a proper association. We guess this is the reason why the basins of attraction are smaller in PCCE than in NM especially when the storage rate is small.

By comparing Figures 4(a) and 5(a), we can see that unstable motions in a failure case are stronger in NM than in PCCE. It seems that PCCE has near equilibrium states that are distant from the target, like spurious memories, when PCCE has a small storage rate ($p/N = 0.25$). The above-mentioned small association ability for a case with a small storage rate also implies the existence of spurious memories. Since the distinction between proper memories and spurious memories is important for an associative memory, this feature might be a defect of our system. In the following, we discuss it further.

Table I shows the overlap and the rate of bitwise flips after a fairly long time for both NM and PCCE. The overlap and the rate of bitwise flips are calculated for successful association results and unsuccessful association results separately. In NM, even after the output becomes equal to the target, fluctuations of the output sometimes remain, as can be seen in Table

I. However, since the output does not veer from the target, such a case is regarded as a successful association. In NM, the number of stored patterns is $0.3N$, the initial overlap is $m(0) = 0.44$, the overlap is averaged in $10.0 \leq t \leq 15.0$, and the rate of bitwise flips is the rate of units that flip in $10.0 \leq t \leq 15.0$. In PCCE, the number of stored patterns is $0.5N$, the initial overlap is $m(0) = 0.6$, the overlap is averaged in $1000 \leq t/4 \leq 1500$, and the rate of bitwise flips is the rate of units that flip in $1000 \leq t/4 \leq 1500$. In the two systems, the initial overlap is set at a little (about 12%) smaller value than the critical overlap (see Figures 12(a) and 12(b)), and the overlap and the flip rate are observed after a fairly long time to make it possible to ignore the transient period. These experimental conditions are determined so that the comparison becomes fair. In NM, the system's internal potential u is updated 1000 times before $t = 10.0$, because the time-interval for the Euler method is 0.01. In PCCE, the internal potential u is updated 1000 times before $t/4 = 1000$.

When PCCE fails to make the association, the overlap is larger and the bitwise flip rate is smaller than those in NM. Namely, unstable motions for failure cases are weaker in PCCE than in NM. These results imply that PCCE has more states that almost equilibrate at a distant position from the target than NM. Nevertheless, especially when PCCE is near memory saturation, i.e., $p \approx 0.58N$, it is possible to discriminate successful association results from unsuccessful results by checking the bitwise flips after the transient period. In the experiment shown in Table I, the flip rate is 0.0 when an association is successful, and it is a positive value when an association is unsuccessful. We can thus discriminate between them, although the difference is not as apparent as in NM. The unstable behavior for an unsuccessful association corresponds to the "I don't know" state (Parisi, 1986; Skarda & Freeman, 1987). It should be noted that the system's stability depends on the parameter β . If β is set at a smaller value, the memory capacity rises to about $0.63N$ at $\beta = 1.0$, though the above-mentioned discrimination becomes less prominent. If β is set at a larger value, the discrimination becomes more prominent, though the memory capacity becomes slightly smaller. We can also observe a similar trade-off phenomenon for parameter κ .

Table I The overlap and the rate of bitwise flips after a long time. In NM, the number of stored patterns is $0.3N$, the initial overlap is $m(0) = 0.44$, the overlap is averaged in $10.0 \leq t \leq 15.0$, and the rate of bitwise flips is the rate of units that flip in $10.0 \leq t \leq 15.0$. In PCCE, the number of stored patterns is $0.5N$, the initial overlap is $m(0) = 0.6$, the overlap is averaged in $1000 \leq t/4 \leq 1500$, and the rate of bitwise flips is the rate of units that flip in $1000 \leq t/4 \leq 1500$. Each overlap value is obtained by averaging the results for at least 100 sets of memory patterns. Each column of the bitwise flip rate shows "average \pm standard deviation" over the sets.

| | | overlap | bitwise flip rate |
|------|---------|---------|-------------------|
| NM | success | 0.999 | 0.002 \pm 0.008 |
| | failure | 0.251 | 0.377 \pm 0.056 |
| PCCE | success | 1.000 | 0.000 \pm 0.000 |
| | failure | 0.560 | 0.114 \pm 0.041 |

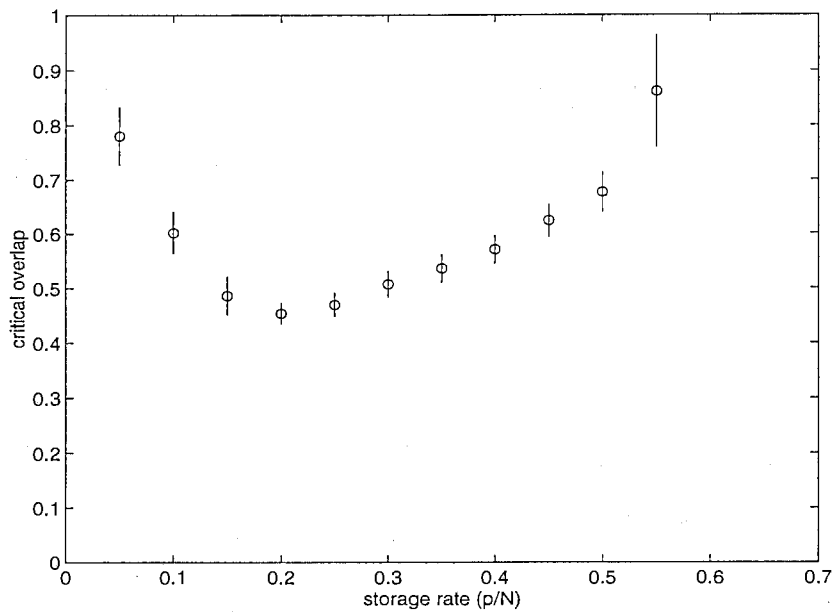


Figure 12(a)

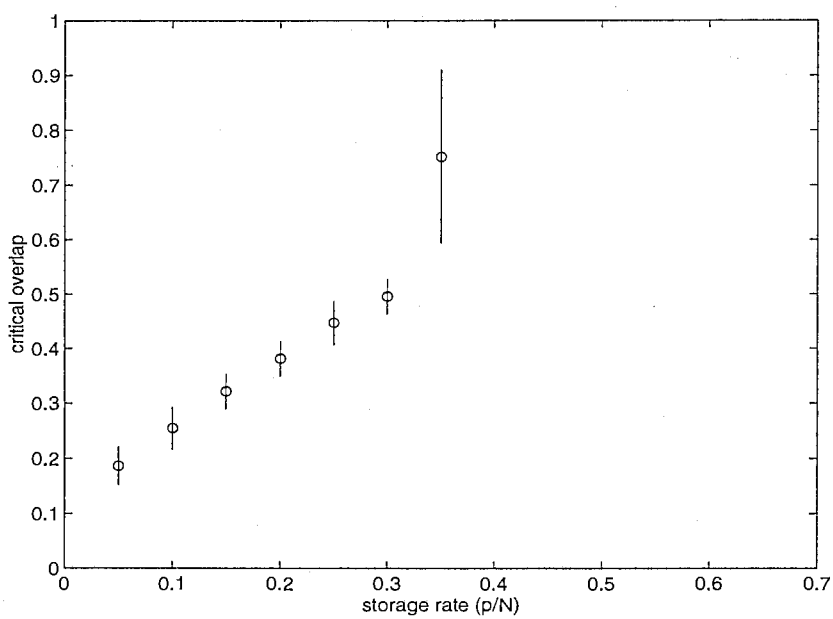


Figure 12(b)

Critical overlap for various storage rate values. Fifty sets of stored patterns were prepared and the first pattern was recalled for each set. The circles and the error bars denote mean values and standard deviations, respectively, for the 50 trials. (a) Critical overlap of PCCE. (b) Critical overlap of NM.

6 Discussion

In the new system PCCE, the dynamics is so improved that its memory capacity becomes much larger than that of the old system \mathcal{CF} . This improvement corresponds to the improvement of NM in comparison with the conventional Hopfield model. Let us discuss here the role of the gain function (8c). For discussion, first, let us consider the reason why a significant improvement is achieved in NM in comparison with the Hopfield model.

In NM, two major improvements are achieved. One is the large memory capacity, and the other is the reduction of spurious memories. First, let us consider the reason why it achieves a large memory capacity. From (10), an equilibrium state \mathbf{x} of the system, which is assumed to correspond to the target memory ξ^1 , is given by

$$x_i = F \left(\xi_i^1 h^1 + \xi_i^2 h^2 + \sum_{k=3}^p \xi_i^k h^k \right). \quad (15)$$

In order to consider the effect of the non-target memory ξ^2 , let us neglect the third term of the internal potential in (15) as a noise term with mean 0. By multiplying both hands of (15) by ξ_i^2/N and summing over i , one can obtain

$$h^2 = (1/N) \sum_{i=1}^N F \left(\xi_i^1 \xi_i^2 h^1 + h^2 \right). \quad (16)$$

Let us assume that ξ^1 and ξ^2 have a correlation c , which means that $\xi_i^1 = \xi_i^2$ for $N(1+c)/2$ units and $\xi_i^1 = -\xi_i^2$ for $N(1-c)/2$ units. Since $h^1 \approx \theta$,

$$\begin{aligned} h^2 &= ((1+c)/2)F(h^1 + h^2) + ((1-c)/2)F(-h^1 + h^2) \\ &= \begin{cases} (c-1)/2 & \text{if } h^2 > 0 \\ (c+1)/2 & \text{if } h^2 \leq 0 \end{cases} \end{aligned} \quad (17)$$

holds. From $-1 \leq c \leq 1$, the possible solution of (17) is $h^2 = 0$, which implies that the correlation between the equilibrium state \mathbf{x} and the non-target memory ξ^2 becomes 0. Namely, the nonmonotonic output function works to orthogonalize the equilibrium state from the non-target memories. This description gives an interpretation for the effect of the nonmonotonic output function, which holds with $p = 2$. However, the small crosstalk variance for a successful association case, which can be observed in Figure 11(c), implies this intuitive interpretation is also true with $p > 2$.

In order to discuss the cases where the number of non-target memories is proportional to N and cannot be neglected, we need the help of the signal-to-noise analysis done by Shiino and Fukai (1993). According to their theory, when the storage rate is relatively small, e.g., $p/N < 0.14$ for $\theta = 0.7$, there is a phase where the crosstalk variance becomes 0. This implies that the correlation between \mathbf{x} and ξ^k ($k > 1$) for a successful association is 0 in the phase. Even when the storage rate is larger than those in the phase, the theory suggests (Okada, *p. c.*) that the crosstalk variance for a successful case is quite small, which has also been confirmed experimentally (Shiino & Fukai, 1993). Further discussion is beyond the scope of this paper.

Next, let us consider the reason why NM achieves a reduction of spurious memories. The Hopfield model with a monotonic output function, i.e., the Heaviside or sigmoidal function, converges to one of the equilibria, which corresponds to either a proper memory or a spurious memory. However, by employing a nonmonotonic output function, some of the equilibria are no longer stable. Therefore, nonmonotonicity works as adding a perturbation to each equilibrium state. With a monotonic output function, it is considered that a proper memory has in general a larger energy barrier between the adjacent equilibrium state than a spurious memory. Therefore, if we add a perturbation to each equilibrium state, spurious memories can become unstable whereas proper memories maintain stability. This reminds us of the reduction of spurious memories in the analog Hopfield model (Hopfield, 1984) compared with the binary model. Ozawa et al. (1994) have theoretically shown that the distribution of spurious states becomes significantly smaller than that of the Hopfield model (Gardner, 1986).

Therefore, a nonmonotonic output function has two roles. It works as an orthogonalization-like mechanism between the effective state \mathbf{x} and the non-target memories ξ^k ($k > 1$), and it makes spurious memories unstable by adding some disturbance to the system state. These improvements are achieved by suppressing the gain of a unit having a large internal potential value in NM.

In our old system \mathcal{CF} defined by (3) and (5), when $(-x_i u'_i)$ is negative, α_i becomes small so that the i th unit becomes stable. Therefore, the system equilibrates at a state where x_i and u'_i have the same sign. This mechanism is almost the same as that in the Hopfield model, implying that there are spurious states also in \mathcal{CF} . In order to expand the memory capacity and to reduce spurious states, we designed the gain function (8c). In (8a), if the internal potential u'_i (8b) has the same sign with x_i and its absolute value is large, the parameter α_i becomes small so that the gain of the i th unit becomes small with the gain function (8c). Therefore, the gain function (8c) suppresses the gain of a unit having a large internal potential value like in NM. Although there are also several remaining effects, including the piecewise linearity of the gain function (8c), the above-mentioned resemblance of the control (8) to the nonmonotonic output function is the most important improvement in PCCE. Thus, with the gain function (8c), the correlation between the system's effective state \mathbf{y} and the non-target memories ξ^k ($k > 1$) becomes small like in NM. This can be seen in Figure 11(d). In addition, the perturbation originating from the gain suppression by (8c) makes the spurious states of \mathcal{CF} unstable, whereas the proper memories maintain stability.

Accordingly, the gain function (8c) of PCCE is similar to the nonmonotonic output function (6b) in NM. It is unclear then why PCCE has a larger memory capacity than that of NM. It is known that the differential equation model with a nonmonotonic output function can have a larger memory capacity if the network has positive self-loops (Morita, 1993; Shiino & Fukai, 1993). However, these positive self-loops produce spurious memories, because they make any states stable. The PCCE's characteristics mentioned in the previous sections, namely, a large memory capacity, relatively small basin volumes, and weak instability in failure cases, suggest that there is a self-stabilizing mechanism similar to that with the positive self-loops. In fact, this observation is partly true. Equation (8a) indicates that if the i th partial energy, $(-x_i u'_i)$, is positive, the bifurcation parameter of the S-MAP becomes large so that the i th unit possibly flips in its output. However, since α_{mid} is set at a smaller value ($= 3.5$) than the band-merge point of the S-MAP (≈ 3.6) there is a hysteresis in this

flip mechanism; if the i th partial energy is positive but small, the i th unit does not flip in its output. Such a hysteresis mechanism is similar to the self-stabilizing mechanism of the positive self-loops. Therefore, some part of the above-mentioned characteristics of PCCE can be attributed to the hysteresis mechanism that is involved in the control of chaos (8a). If the parameter α_{mid} is set at a larger value, e.g., $\alpha_{mid} = 3.6$, the effect of the hysteresis disappears so that the memory capacity becomes small, the basin volumes for the small storage rate cases expand, and the instability in failure cases becomes large. Figure 13 shows the experimental results of the critical overlap for $\alpha_{mid} = 3.6$, which shows that a PCCE with that parameter value has a memory capacity of $0.40N$ and large basin volumes for a small storage rate.

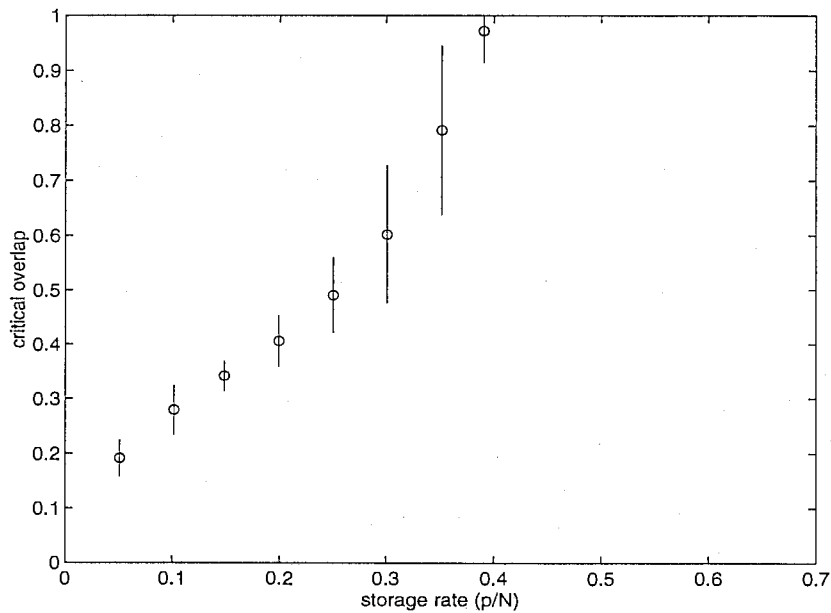


Figure 13

Critical overlap of PCCE for various storage rate values. Parameters are set at $\alpha_{mid} = 3.6$ and $\alpha_{min} = 3.2$. The other parameters are the same as those in Figure 12(a). Fifty sets of stored patterns were prepared and the first pattern was recalled for each set. The circles and the error bars denote mean values and standard deviations, respectively, for the 50 trials.

In our associative memory system PCCE, memories are stored by means of a condensed autocorrelation matrix, i.e., Hebbian learning. When the system encounters an initial state that is close to one of the stored memories, the system searches for the proper memory with strong chaotic motions in the early association stage. When the system can successfully recall a proper memory, the system almost equilibrates in a spatially coherent oscillation, while localized chaotic motions remain. When the system fails to make the association, the chaotic motions are large enough to become non-localized, which corresponds to the “I don’t know” state. Especially when the system is near memory saturation, successful association results can be discriminated from unsuccessful results, by checking the existence of such non-localized chaotic motions. Furthermore, our new system has a large memory capacity due to the nonlinear gain function. The gain function suppresses the gain of a unit whose internal potential is large, i.e., its chaos is weak.

7 Conclusion

We previously proposed an associative memory system \mathcal{CF} , which has a larger memory capacity and larger basin volumes than the Hopfield model employing the same autocorrelational learning scheme. This implies that the chaotic dynamics employed in our system is more efficient than the relaxation dynamics employed in the Hopfield model. Nevertheless, even in \mathcal{CF} , spurious memories do exist. In this paper, we aim to reduce the spurious memories modifying its dynamics and to expand the memory capacity.

Intuitively, a spurious memory occurs due to the correlation between the retrieval state and the non-target memories. Therefore, if one can lower the correlation, spurious memories can be reduced. In addition, the low correlation makes the retrieval state corresponding to the target memory stable, so the memory capacity can be expanded. In the differential equation model with a nonmonotonic output function, the correlation lowering is achieved by suppressing the gain of a unit with a large internal potential value. This control corresponds to the gain suppression of a unit with a low chaos parameter in our new system, PCCE. Experiments also show that our new dynamics achieves the correlation reduction. Therefore, PCCE has a large memory capacity, which is estimated at $0.58N$. In addition, especially when PCCE is near memory saturation, we can discriminate between successful association results and unsuccessful results by checking the existence of non-localized unstable motions. When the system successfully recalls the target memory, the system’s motion is dominated by a spatially coherent oscillation with some localized chaotic motions, while non-localized chaotic motions remain as the “I don’t know” state when the system fails to make the association. This discrimination is very important for an associative memory system. If the discrimination is not necessary, the memory capacity can be raised to about $0.63N$ by setting the parameter β at 1.0.

References

- [1] Aihara, K., Takabe, T., & Toyoda, M. (1990). Chaotic neural networks. *Physics Letters A*, **144**, 333-340.
- [2] Amari, S. (1972a). Characteristics of random nets of analog neuron-like elements. *IEEE Transactions on Systems, Man, and Cybernetics*, **SMC-2**, 643-657.
- [3] Amari, S. (1972b). Learning patterns and pattern sequences by self-organizing nets of threshold elements. *IEEE Transactions on Computers*, **C-21**, 1197-1206.
- [4] Amari, S., & Maginu, K. (1988). Statistical neurodynamics of associative memory. *Neural Networks*, **1**, 63-73.
- [5] Amari, S. (1989). Characteristics of sparsely encoded associative memory. *Neural Networks*, **2**, 451-457.
- [6] Amit, D. J., Gutfreund, H., & Sompolinsky, H. (1985a). Spin-glass models of neural networks. *Physical Review A*, **32**, 1007-1018.
- [7] Amit, D. J., Gutfreund, H., & Sompolinsky, H. (1985b). Storing infinite numbers of patterns in a spin-glass model of neural networks. *Physical Review Letters*, **55**, 1530-1533.
- [8] Anderson, J. A. (1972). A simple neural network generating an interactive memory. *Mathematical Biosciences*, **14**, 197-220.
- [9] Babcock, K. L., & Westervelt, R. M. (1987). Dynamics of simple electronic neural networks. *Physica D*, **28**, 305-316.
- [10] Babloyantz, A., & Destexhe, A. (1986). Low-dimensional chaos in an instance of epilepsy. *Proceedings of the National Academy of Sciences, USA*, **83**, 3513-3517.
- [11] Baird, B. (1986). Nonlinear dynamics of pattern formation and pattern recognition in the rabbit olfactory bulb. *Physica D*, **22**, 150-175.
- [12] Coolen, A. C. C., & Sherrington, D. (1993). Dynamics of fully connected attractor neural networks near saturation. *Physical Review Letters*, **71**, 3886-3889.
- [13] Eckhorn, R., Bauer, R., Jordan, M., Brosch, M., Kruse, W., Munk, M., & Reitboeck, H. J. (1988). Coherent oscillations: A mechanism of feature linking in the visual cortex? Multiple electrode and correlation analyses in the cat. *Biological Cybernetics*, **60**, 121-130.
- [14] Freeman, W. J., Yao, Y., & Burke, B. (1988). Central pattern generating and recognizing in olfactory bulb: A correlation learning rule. *Neural Networks*, **1**, 277-288.
- [15] Gardner, E. (1986). Structure of metastable states in the Hopfield model. *Journal of Physics A: Mathematical and General*, **19**, L1047-L1052.

- [16] Gray, C. M., Singer, W. (1989). Stimulus-specific neuronal oscillations in orientation columns of cat visual cortex. *Proceedings of the National Academy of Science, USA*, **86**, 1698-1702.
- [17] Grossberg, S., & Somers, D. (1991). Synchronized oscillations during cooperative feature linking in a cortical model of visual perception. *Neural Networks*, **4**, 453-466.
- [18] Hayashi, Y. (1994). Oscillatory neural network and learning of continuously transformed patterns. *Neural Networks*, **7**, 219-231.
- [19] Hertz, J., Krogh, A., & Palmer, R. G. (1991). *Introduction to the Theory of Neural Computation*. Redwood City: Addison-Wesley.
- [20] Holden, A. V., Winlow, W., & Haydon, P. G. (1982). The induction of periodic and chaotic activity in a molluscal neurone. *Biological Cybernetics*, **43**, 169-173.
- [21] Hopfield, J. J. (1982). Neural networks and physical systems with emergent collective computational abilities, *Proceedings of the National Academy of Sciences, USA*, **79**, 2554-2558.
- [22] Hopfield, J. J. (1984). Neurons with graded responses have collective computational properties like those of two-state neurons. *Proceedings of the National Academy of Science USA*, **81**, 3088-3092.
- [23] Inoue, M., & Nagayoshi, A. (1991). A chaos neuro-computer. *Physics Letters A*, **158**, 373-376.
- [24] Ishii, S., Fukumizu, K., & Watanabe, S. (1996). A network of chaotic elements for information processing. *Neural Networks*, **9**, 25-40.
- [25] Ishii, S. Eliminating spurious memories in a network of chaotic elements. *Journal of Intelligent & Fuzzy Systems*, (to appear). also in *ATR Technical Report, TR-H-106*, Kyoto: ATR.
- [26] Kaneko, K. (1989). Pattern dynamics in spatiotemporal chaos: Pattern selection, diffusion of defect and pattern competition intermittency. *Physica D*, **34**, 1-41.
- [27] Kaneko, K. (1990). Clustering, coding, switching, hierarchical ordering, and control in a network of chaotic elements. *Physica D*, **41**, 137-172.
- [28] Kaneko, K. (1992). Mean field fluctuation in network of chaotic elements. *Physica D*, **55**, 368-384.
- [29] Kanter, I., & Sompolinsky, H. (1987). Associative recall of memory without errors. *Physical Review A*, **35**, 380-392.
- [30] Kohonen, T. (1972). Correlation matrix memories. *IEEE Transactions on Computers*, **C-21**, 353-359.

- [31] Kohonen, T. (1977). *Associative Memory - A System-Theoretical Approach*, Berlin: Springer-Verlag.
- [32] König, P., & Schillen, T. B. (1991). Stimulus-dependent assembly formation of oscillatory responses: I. Synchronization. *Neural Computation*, **3**, 155-166.
- [33] Kühn, R., Bös, S., & Hemmen, J. L. (1991). Statistical mechanics for networks of graded-response neurons. *Physical Review A*, **43**, 2084-2087.
- [34] Kuramoto, Y. (1991). Collective synchronization of pulse-coupled oscillators and excitable units. *Physica D*, **50**, 15-30.
- [35] Li, Z., & Hopfield, J. J. (1989). Modeling the olfactory bulb and its neural oscillatory processing. *Biological Cybernetics*, **61**, 379-392.
- [36] Lumer, E. D., & Huberman, B. A. (1992). Binding hierarchies: A basis for dynamic perceptual grouping. *Neural Computation*, **4**, 341-355.
- [37] Matsumoto, G., Aihara, K., Hanyu, Y., Takahashi, N., Yoshizawa, S., & Nagumo, J. (1987). Chaos and phase locking in normal squid axons. *Physics Letters A*, **123**, 162-166.
- [38] McEliece, R. J., Posner, E. C., Rodemich, E. R., & Venkatesh, S. S. (1987). The capacity of the Hopfield associative memory. *IEEE Transactions on Information Theory*, **33**, 461-482.
- [39] Morita, M. (1993). Associative memory with nonmonotone dynamics. *Neural Networks*, **6**, 115-126.
- [40] Nakano, K. (1972). Associatron - A model of associative memory. *IEEE Transactions on Systems, Man, and Cybernetics*, **SMC-2**, 380-388.
- [41] Nara, S., Davis, P., & Totsuji, H. (1993). Memory search using complex dynamics in a recurrent neural network model. *Neural Networks*, **6**, 963-973.
- [42] Okada, M. (1995). A hierarchy of macrodynamical equations for associative memory. *Neural Networks*, **8**, 833-838.
- [43] Okada, M. private communication.
- [44] Ozawa, K., Fukai, T., Shiino, M., & Ohba, I. (1994). The distribution of the metastable states in neural networks of non-monotonic neurons. *Abstracts of the Meetings of the Physical Society of Japan*, **49**(3), 569. (in Japanese).
- [45] Palm, G. (1980). On associative memory. *Biological Cybernetics*, **36**, 19-31.
- [46] Parisi, G. (1986). Asymmetric neural networks and the process of learning. *Journal of Physics A: Mathematical and General*, **19**, L675-L680.
- [47] Peretto, P. (1988). On learning rules and memory storage abilities of asymmetrical neural networks. *Journal de Physique*, **49**, 711-726.

- [48] Peterson, C., & Anderson, J. R. (1987). A mean field theory learning algorithm for neural networks. *Complex Systems*, **1**,
- [49] Peterson, C., & Hartman, E. (1989). Explorations of the mean field theory learning algorithm. *Neural Networks*, **2**, 475-494.
- [50] Riedel, U., Kühn, R., & van Hemmen, J. L. (1988). Temporal sequences and chaos in neural nets. *Physical Review A*, **38**, 1105-1108.
- [51] Sato, M. (1994). The asynchronous MFT equation converges faster than the Hopfield network. *ATR Technical Report, TR-H-089*, Kyoto: ATR.
- [52] Schillen, T. B., & König, P. (1991). Stimulus-dependent assembly formation of oscillatory responses: II. Desynchronization. *Neural Computation*, **3**, 167-178.
- [53] Sherrington, D., & Kirkpatrick, S. (1975). Solvable model of a spin-glass. *Physical Review Letters*, **35**, 1792-1796.
- [54] Shiino, M., & Fukai, T. (1990). Replica-symmetric theory of the nonlinear analog neural networks. *Journal of Physics A: Mathematical and General*, **23**, L1009-L1017.
- [55] Shiino, M., & Fukai, T. (1993). Self-consistent signal-to-noise analysis of the statistical behavior of analog neural networks and enhancement of the storage capacity. *Physical Review E*, **48**, 867-897.
- [56] Skarda, C. A., & Freeman, W. J. (1987). How brains make chaos in order to make sense of the world. *Behavioral and Brain Sciences*, **10**, 161-195.
- [57] Sompolinsky, H., Kanter, I. (1986). Temporal association in asymmetric neural networks. *Physical Review Letters*, **57**, 2861-2864.
- [58] Sompolinsky, H., Crisanti, A., & Sommers, H. J. (1988). Chaos in random neural networks. *Physical Review Letters*, **61**, 259-262.
- [59] Treves, A., & Rolls, E. T. (1992). Computational constraints suggest the need for two distinct input systems to the hippocampal CA3 network. *Hippocampus*, **2**, 189-199.
- [60] Tsuda, I. (1992). Dynamic link of memory - Chaotic memory map in nonequilibrium neural networks, *Neural Networks*, **5**, 313-326.
- [61] Wang, D., Buhmann, J., & von der Malsburg, C. (1990). Pattern segmentation in associative memory. *Neural Computation*, **2**, 94-106.
- [62] Weisbuch, G., & Fogelman-Soulié, F. (1985). Scaling laws for the attractors of Hopfield networks. *Journal de Physique Letters*, **46**, 623-630.
- [63] Yao, Y., & Freeman, W. J. (1990). Model of biological pattern recognition with spatially chaotic dynamics. *Neural Networks*, **3**, 153-170.
- [64] Yoshizawa, S., Morita, M., & Amari, S. (1993). Capacity of associative memory using a nonmonotonic neuron model. *Neural Networks*, **6**, 167-176.